From bare interactions, low-energy constants, and unitary gas to nuclear density functionals without free parameters: Application to neutron matter

Denis Lacroix,* Antoine Boulet, Marcella Grasso, and C.-J. Yang
Institut de Physique Nucléaire, IN2P3-CNRS, Université Paris-Sud, Université Paris-Saclay, F-91406 Orsay Cedex, France
(Received 3 February 2017; published 9 May 2017)

We further progress along the line of Ref. [D. Lacroix, Phys. Rev. A **94**, 043614 (2016)] where a functional for Fermi systems with anomalously large s-wave scattering length a_s was proposed that has no free parameters. The functional is designed to correctly reproduce the unitary limit in Fermi gases together with the leading-order contributions in the s- and p-wave channels at low density. The functional is shown to be predictive up to densities $\sim$0.01 fm^{-3} that is much higher densities compared to the Lee-Yang functional, valid for $\rho < 10^{-6}$ fm^{-3}. The form of the functional retained in this work is further motivated. It is shown that the new functional corresponds to an expansion of the energy in $(a_s k_F)$ and $(r_e k_F)$ to all orders, where r_e is the effective range and k_F is the Fermi momentum. One conclusion from the present work is that, except in the extremely low-density regime, nuclear systems can be treated perturbatively in $-(a_s k_F)^{-1}$ with respect to the unitary limit. Starting from the functional, we introduce density-dependent scales and show that scales associated with the bare interaction are strongly renormalized by medium effects. As a consequence, some of the scales at play around saturation are dominated by the unitary gas properties and not directly by low-energy constants. For instance, we show that the scale in the s-wave channel around saturation is proportional to the so-called Bertsch parameter ξ_0 and becomes independent of a_s. We also point out that these scales are of the same order of magnitude than those empirically obtained in the Skyrme energy density functional. We finally propose a slight modification of the functional such that it becomes accurate up to the saturation density $\rho \simeq 0.16$ fm^{-3}.

DOI: 10.1103/PhysRevC.95.054306

I. INTRODUCTION

In the last 50 years, nuclear theoretical physics has encountered two major breakthroughs. The first one was the nuclear density functional theory (DFT) approach also called energy density functional (EDF) theory. In the 1970s, it was realized that simple functionals [1–3] based on the concept of effective interaction can be very accurate while simultaneously unifying the description of nuclear structure [4,5], nuclear dynamics [6,7] or thermodynamics [8]. Nuclear EDF remains, even today, the only microscopic approach able to describe nuclear systems from small masses ($N \geqslant 16$) to infinite nuclear matter. Still, the understanding of *"why functional of extreme simplicity can work so well despite the known complexity of the underlying many-body interaction"* remains unclear.

A second breakthrough was made more recently on the nuclear interaction itself and on its application to nuclear systems. In particular, it was realized that the strong nuclear repulsion at short distances can be replaced by a softer potential that is optimized for the low-energy scales relevant for nuclei [9,10]. Progress was made along this line in previous decades, especially under the impulse of the nuclear effective field theory (EFT) leading to a constructive approach [11–17] for the nucleon-nucleon interaction. The possibility of getting rid of the strong repulsion turns out to considerably simplify the nuclear many-body problem. In particular, nuclei become more perturbative and methods that were extremely difficult to apply with former generations of bare interactions become manageable. Considerable efforts are made nowadays to develop accurate exact calculations, called *ab initio* methods, for infinite matter and nuclei [10,18–20]. A very important aspect of the strategy used in *ab initio* methods is that the complexity of the nuclear interaction is gradually increased using power counting analysis leading to exact calculations with controlled errors. One difficulty that is encountered is that the EFT approach automatically leads to three-body and more generally many-body interactions that are not easy to handle in applications. Nevertheless, by treating the Lagrangian at increasing orders, one should reduce gradually the error bars in exact calculations. One can note, however, that in practice error bars do not decrease so fast from LO to N2LO or N3LO, etc. In addition, when applying *ab initio* methods to infinite systems, these error bars are increasing with density (small relative distances), as expected, and turn out to be somewhat large around the saturation density (see, for instance, [21]).

Quite naturally, attempts have been made to take advantage of this progress on the nuclear interaction and to obtain less empirical nuclear EDF. This includes the use of density matrix expansion (DME) [22–27] or functionals deduced, for instance, in infinite systems, like in the ongoing effort summarized in Ref. [12]. Another path that is now explored is to clarify the notion of beyond mean-field approaches within EDF and eventually propose new functionals using techniques from EFT [28–30]. A common feature of these attempts is that the functionals become rapidly complicated and therefore are at variance with the apparent simplicity of more empirical nuclear EDF.

Alternatively, it was noted that because of the very large s-wave scattering length of the nuclear interaction, nuclear systems are expected to be close to unitary gas where the scattering length becomes infinitely large. Numerous experimental

*lacroix@ipno.in2p3.fr

and theoretical works have been made on the unitary regime [31–33]. Unitary gases are universal in the sense that, independently from the original interaction and particles nature, the energy can be written as $E = \xi_0 E_{\rm FG}$ where ξ_0 is the so-called Bertsch parameter [34] and $E_{\rm FG}$ is the free gas energy. In view of this, minimalist functionals have been produced at unitarity [33,35,36].

Our primary goal is to construct simple functionals for neutron matters with as less free parameters as possible, rendering the functionals at the same time less empirical. The starting point in the recent work [37] is to use the universality of unitary gas on one side and the behavior of nuclear systems at very low density to propose a new functional. Here, we report new progress we have made along this line. A more precise discussion and justification of the functional form we have retained is made. The functional is finally further improved by imposing that the effective-range dependence of the unitary gas is better reproduced.

The novel functional leads naturally to density-dependent scales that identify with the bare scales at very low density and strongly evolve with the density. We show that the scale obtained in this way helps to understand why empirical functionals like Skyrme-based EDF, although very simple and not connected to the bare interaction can be so predictive (see Sec. IV).

II. PARAMETER-FREE NUCLEAR DENSITY FUNCTIONALS

Following the recent work of Ref. [37], we focus here on neutron matter. We consider a spin-degenerate system interacting through an s-wave interaction characterized by its phase shift δ_0 at low momentum transfer:

$$k \cot \delta_0 = -\frac{1}{a_s} + \frac{1}{2} r_e k^2 + O(k^4). \tag{1}$$

where k is the relative momentum of the interacting particles and where the low-energy constants (LECs) a_s and r_e stand, respectively, for the s-wave scattering length and the effective range. For neutron matter, these low-energy constants are equal to $a_s = -18.9$ fm and $r_e = 2.7$ fm.

Guided by the resummation technique used in low-density Fermi gases with large scattering length [38–40] and on the recent efforts to develop a nuclear energy density functional correctly treating low-density Fermi liquids [41], a novel density functional for neutron matter was proposed in Ref. [37]. This functional can be generically written as

$$\frac{E}{E_{\rm FG}} = \xi(a_s k_F, r_e k_F), \tag{2}$$

where $E_{\rm FG}$ is the free Fermi gas energy given by $E_{\rm FG}/N = 3\hbar^2 k_F^2/(10m)$. Here N is the number of particles, and k_F is the Fermi momentum that is obtained from the single-particle density ρ through $\rho = \nu k_F^3/(6\pi^2)$. ν is the degeneracy ($\nu = 2$ for neutron matter). In Ref. [37], the following ξ functional was proposed:

$$\xi(a_s k_F, r_e k_F) = 1 + \frac{5}{3} \frac{(a_s k_F) A_0}{1 - A_0^{-1}[A_1 + (r_e k_F) A_2] a_s k_F}. \tag{3}$$

In addition to this specific form, an important aspect is that the parameters $\{A_i\}$ are not adjustable but are fixed by imposing well-defined limits.

One possibility that was explored in Refs. [39,41] is to fix some parameters by imposing the correct low–density limit. In general, the energy of a Fermi system can be written as

$$\frac{E}{E_{\rm FG}} = 1 + \frac{E^{(1)}}{E_{\rm FG}} + \frac{E^{(2)}}{E_{\rm FG}} + \cdots, \tag{4}$$

where $E^{(1)}$ is the Hartree-Fock energy, $E^{(2)}$ (respectively, $E^{(n)}$) is the second-order (respectively, $n^{\rm th}$ order) perturbation theory contribution. At low density, the different contributions can be expanded in power of k_F as [42]:[1]

$$\frac{E^{(1)}}{E_{\rm FG}} = \frac{10}{9\pi}(\nu - 1)(k_F a_s) + (\nu - 1)\frac{1}{6\pi}(k_F r_e)(k_F a_s)^2 + (\nu + 1)\frac{1}{3\pi}(k_F a_p)^3 + \cdots, \tag{5}$$

$$\frac{E^{(2)}}{E_{\rm FG}} = (\nu - 1)\frac{4}{21\pi^2}(11 - 2\ln 2)(k_F a_s)^2 + \cdots. \tag{6}$$

We recognize in particular some of the terms appearing in the Lee-Yang formula obtained in Refs. [44–46]. Setting the p-wave scattering volume to zero and imposing to recover the different terms appearing in Eqs. (5) and (6) when Taylor expanding (3) to second order in $(a_s k_F)$ and first order in $(r_e k_F)$ provides a unique determination of the A_i parameters (see [37] for explicit values). Results of this method are shown in Figs. 1(a) and 1(b). As noted in Refs. [37,39], these results are actually not so far from the exact QMC at low density even if $-(a_s k_F) \gg 1$.

As an alternative strategy, starting from the fact that the s-wave scattering length in nuclear matter is very large, it was proposed to constrain the functional (3) keeping the constraint of the Hartree-Fock expansion, Eq. (5), while using the unitary gas limit instead of the second-order contribution. The unitary regime corresponds to the limit $-(a_s k_F)^{-1} \to 0$. After simple manipulations, the unitary gas limit is better emphasized by rewriting Eq. (3) as

$$\frac{E}{E_{\rm FG}} = 1 - \frac{U_0}{1 - (a_s k_F)^{-1} U_1} + \frac{R_0(r_e k_F)}{[1 - R_1 (a_s k_F)^{-1}][1 - R_1 (a_s k_F)^{-1} + R_2 (r_e k_F)]}, \tag{7}$$

where new parameters can be expressed in terms of the original A_i coefficients.[2] In Ref. [37], the three independent parameters have been adjusted by imposing that the leading order in

[1] Note that these expressions are valid if pairing correlations are neglected. The presence of pairing estimated using the Hartree-Fock-Bogolyubov approach [42] would lead to an additional contribution associated, for instance, in the s-wave channel to a pairing gap $\Delta \propto \exp(-\pi/[2k_F|a_s|])$ [43].

[2] It can be shown that starting from Eq. (3), we have the relationships $U_1 = R_1$ and $R_0 = U_0 R_2$, so that the number of independent parameters in (7) is the same as in (3). However, in the present study,

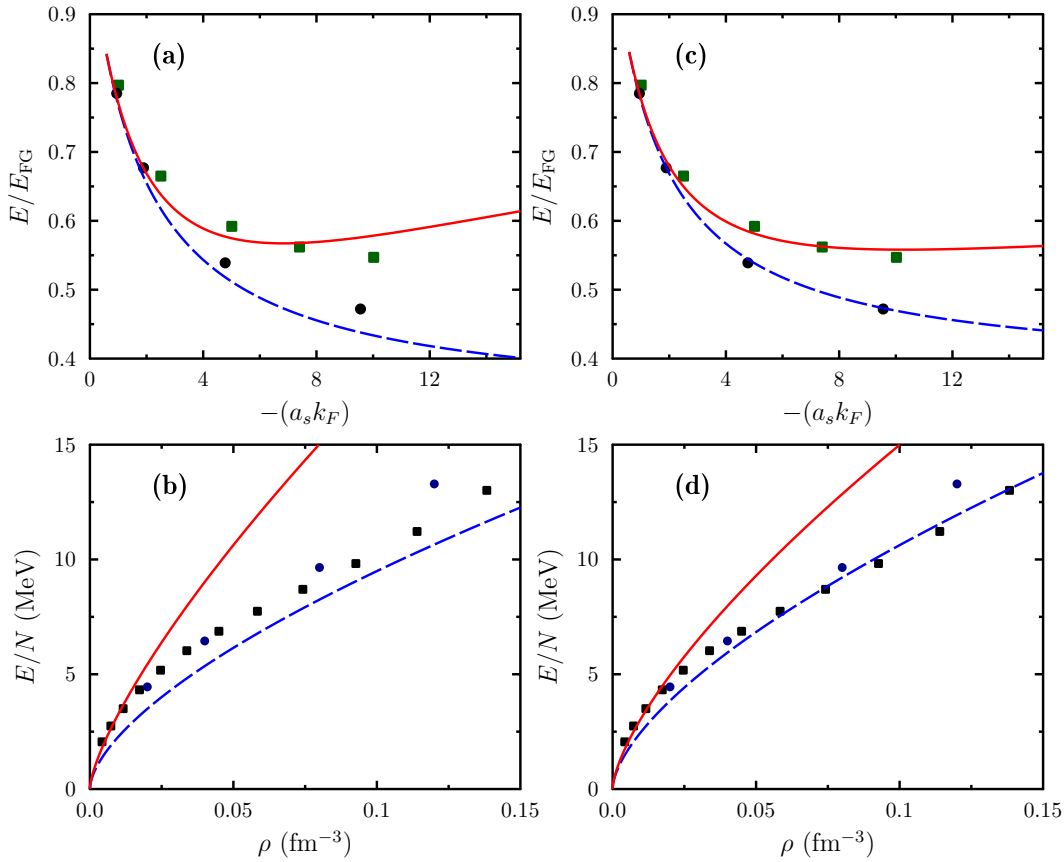

FIG. 1. Neutron matter energy as a function either of $-(a_s k_F)$ or ρ. (a) and (b) show the results to the results obtained by using Eq. (3) where the A_i coefficients are adjusted by imposing the developments given by Eqs. (5) and (6). (c) and (d) show the results of Eq. (7) where U_i and R_i are obtained using Eq. (5) and unitarity limits as constraints. In all panels, the red solid lines correspond to the equation of state including the effective-range dependence while the blue dashed lines correspond to the result obtained by assuming $r_e = 0$. In (a) and (c), the black circles and green squares correspond to the QMC results of Refs. [47,48], respectively, for the cold atom case and AV4 (s-wave only) case. In (b) and (d), the black squares and dark blue circles correspond, respectively, to the *ab initio* results of Refs. [49,50]. Note finally that the highest density shown in the upper panels corresponds to $\rho = 0.01$ fm^{-1} and corresponds to a very narrow region of (b) and (d).

the low-density expansion in $(a_s k_F)$ and the behavior of the quantity $E/E_{\rm FG}$ at unitarity are correctly reproduced. More precisely, we took advantage of the recent study [51] where the possible effect of nonzero effective range in unitary gases was analyzed:

$$\xi(+\infty, r_e k_F) \equiv \xi_0 + (r_e k_F)\eta_e + (r_e k_F)^2 \delta_e. \tag{8}$$

ξ_0 is the Bertsch parameter while η_e and δ_e are two new parameters. In the present work, we take the reference values $\xi_0 = 0.376$, $\eta_e = 0.127$, and $\delta_e = -0.055$ [51]. It is worth mentioning that these values correspond to averages over the different interactions considered in Ref. [51]. We tested the sensitivity of the result to the η_e value (assuming $\delta_e = 0$). Reducing η_e to 0.046 as originally obtained in Ref. [52] gives a slightly lower energy at low density while the shape and order of magnitude of the energy is globally unchanged for the density considered in Fig. 1(d).

In our previous work, accounting for the constraints between the U_i and R_i, three constraints were necessary to fix the three independents parameters. Then, only ξ_0 and η_e where used as a constraint [37] together with the correct leading order (LO) in $(a_s k_F)$ at low density. Here we slightly improve the functional by directly using expression (7) and relax the constraints between the different U_i and R_i coefficients. Then five constraints are needed to fix the five parameters. We impose that the three terms of Eq. (8) are reproduced as well as the second and third terms of Eq. (5). This gives

$$\begin{cases} U_0 = (1-\xi_0) = 0.62400, \\ U_1 = \frac{9\pi}{10}(1-\xi_0) = 1.76432, \\ R_0 = \eta_e = 0.12700, \\ R_1 = \sqrt{\frac{6\pi\eta_e}{(v-1)}} = 1.54722, \\ R_2 = -\delta_e/\eta_e = 0.43307. \end{cases} \tag{9}$$

Results of the functional (7) are shown in Figs. 1(c) and 1(d).

In Fig. 1(c), we also display the result obtained with the functional (7) assuming $r_e = 0$ (blue dashed line) and compare it with the QMC calculations obtained in Refs. [47,48] (solid circles). In this case, the functional only depends on the two

we will not impose this constraint and simply fix the five parameters entering in Eq. (7) independently from each other.

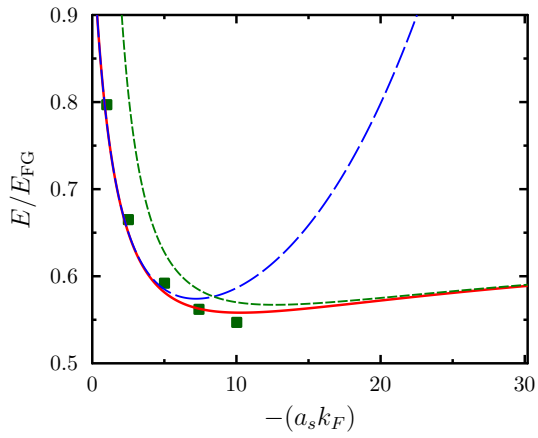

FIG. 2. Same as Fig. 1(c). The green squares correspond to QMC results of Ref. [47] and the red solid line to results of Eq. (7). The green short dashed line and blue long dashed line correspond to the expansion of Eq. (7) to first order in $(a_s k_F)^{-1}$ or to first order in $(r_e k_F)$, respectively.

parameters U_0 and U_1 that are both only functions of the Bertsch parameter ξ_0. Despite its simplicity the functional result perfectly matches the exact QMC result. As noted in Ref. [37], it confirms the finding of Refs. [53,54] where a similar functional was proposed at unitarity.

By comparing the two red lines displayed, respectively, in Figs. 1(a) and 1(b) with the QMC results in neutron matter (solid squares), we also note that taking the constraint on the unitary limit instead of the constraint to reproduce the term appearing in (6) significantly improves the description of neutron matter. From this, it seems quite clear that the unitary gas regime is a good starting point.To illustrate how perturbative neutron matter is with respect to unitary gas and/or low-density regime, we show in Fig. 2 the results of first-order Taylor expansion of Eq. (7) either in $(a_s k_F)^{-1}$ or in $(r_e k_F)$. It is then clear that the former expansion rapidly converges to the full expression. In particular, at densities above $\rho = 0.01$ fm^{-3}, the first-order expansion in $(a_s k_F)^{-1}$ cannot be distinguished from the result of Eq. (7). It is interesting also to mention that the first-order expansion in $(r_e k_F)$ deviates somewhat fast from the function (7). Indeed, although r_e is much smaller than $|a_s|$, for densities around the saturation density of symmetric matter, we are beyond the range of validity of an expansion in the effective range. It can also be stressed that Eq. (7) contains all orders in $(r_e k_F)$ and therefore can also be seen as a resummed expression accounting for effective-range effects. This aspect is discussed below.

III. MEAN-FIELD BASED ON FINITE-RANGE INTERACTION: DISCUSSION OF RESUMMATION OF EFFECTIVE-RANGE EFFECT

In Ref. [37], the effective-range dependence of the unitary gas regime was introduced without much justifying the retained expression. Here, we would like to give more physical insight in the expression and to show that the effective-range dependence entering in (3) can be also regarded as a resummation of r_e effect. The easiest way to introduce effective-range effects beyond those contained in Eq. (5) is to consider the Hartree-Fock energy associated with a finite-range interaction. We take below the case of a Gaussian interaction. This section also illustrates how the interaction parameters should be adjusted to properly account for the low-energy constants coming from the underlying Lagrangian. This strategy is very similar to what is usually done in EFT. The connection with EFT based on zero range interaction is then naturally made here. Finally, a discussion on the possibility of making resummation of the effective range such that the functional (3) is recovered.

A. Preliminary: Hartree-Fock energy of a Gaussian two-body interaction

We consider here a two-body Gaussian interaction written in the form,

$$v(\mathbf{r}_1,\mathbf{r}_2) = \{v_0 + v_\sigma P_\sigma\} g(\mathbf{r}_1 - \mathbf{r}_2), \tag{10}$$

where v_0 and v_σ are parameters. P_σ is the operator that exchanges the spin of two particles and g is a normalized Gaussian given by

$$g(r) = \frac{e^{-(r^2/\mu^2)}}{(\mu\sqrt{\pi})^3}, \tag{11}$$

where $r = |\mathbf{r}_1 - \mathbf{r}_2|$ and μ is a free parameter. The Hartree-Fock contribution of this interaction to the equation of state of neutron matter gives

$$\frac{E_G^{(1)}}{N} = \frac{\rho}{2}[A - BF(\mu k_F)], \tag{12}$$

where A and B are

$$A = v_0 + \tfrac{1}{2}v_\sigma, \quad B = \tfrac{1}{2}v_0 + v_\sigma. \tag{13}$$

F is a function given by

$$F(x) = \frac{4}{\sqrt{\pi}x^3}\int_0^{+\infty} z^2 e^{-z^2/x^2}\left(\frac{3j_1(z)}{z}\right)^2 dz, \tag{14}$$

$$= \frac{12}{x^6}(1 - e^{-x^2}) + \frac{6}{x^4}(e^{-x^2} - 3) + \frac{6\sqrt{\pi}}{x^3}\mathrm{Erf}(x), \tag{15}$$

where $j_1(z)$ denotes the spherical Bessel function and $x = \mu k_F$.

B. Discussion on the low-density limit and relation between the EFT, Skyrme, and Gaussian interaction parameters

Fermi systems at low density have been widely studied using the EFT approach based on a zero-range interaction. In that case, spin-degenerate systems can be studied using a two-body interaction written in the form [46],

$$\langle \mathbf{k}|V_{\rm EFT}|\mathbf{k}'\rangle = C_0 + \frac{C_2}{2}(\mathbf{k}^2 + \mathbf{k}'^2) + C_2'\mathbf{k}.\mathbf{k}', \tag{16}$$

or equivalently in r space,

$$v(\mathbf{r}_1,\mathbf{r}_2) = C_0\delta(\mathbf{r}_1-\mathbf{r}_2) + \tfrac{1}{2}C_2[\delta(\mathbf{r}_1-\mathbf{r}_2)\mathbf{k}^2 + \mathbf{k}'^2\delta(\mathbf{r}_1-\mathbf{r}_2)] + C_2'\mathbf{k}'\delta(\mathbf{r}_1-\mathbf{r}_2)\mathbf{k}'. \quad (17)$$

Using this interaction, the Hartree-Fock energy then read

$$\frac{E}{N} = \frac{3}{5}\frac{\hbar^2k_F^2}{2m} + \frac{k_F^3}{4\pi^2}\left(\frac{C_0}{3} + \frac{k_F^2}{10}[(\nu-1)C_2 + (\nu+1)C_2']\right). \quad (18)$$

At low-density, we can then compare to the Hartree-Fock contribution given in Eq. (5). The low-density expansion of the HF energy is recovered under the condition that the parameters C_i are linked to the low-energy constants through [46]

$$C_0 = \frac{4\pi\hbar^2}{m}a_s,\ C_2 = \frac{2\pi\hbar^2}{m}r_e a_s^2,\ C_2' = \frac{4\pi\hbar^2}{m}a_p^3. \quad (19)$$

a_p^3 is the so-called p-wave scattering volume. [3] Similarly to the EFT case based on zero-range interaction, one can recover the low-density expression starting from the Gaussian interaction. The most direct way to make connections between Eq. (10) and Eqs. (17) and (18) is to expand the interaction in terms of the momentum transferred. Starting from Eq. (10) and expanding in $(\mathbf{k}-\mathbf{k}')$ up to second order, we have

$$v(\mathbf{k},\mathbf{k}') = (v_0 + v_\sigma P_\sigma)\left(1 - \frac{\mu^2}{4}[\mathbf{k}^2 + \mathbf{k}'^2]\right) + \frac{1}{2}\mu^2(v_0 + v_\sigma P_\sigma)\mathbf{k}.\mathbf{k}' + \cdots. \quad (21)$$

Making the inverse Fourier transform, one then obtains the Skyrme-type interaction with standard (x_i,t_i) parameters:

$$v(\mathbf{r}_1,\mathbf{r}_2) = t_0(1+x_0P_\sigma)\delta(\mathbf{r}_1-\mathbf{r}_2) + \frac{1}{2}t_1(1+x_1P_\sigma)[\delta(\mathbf{r}_1-\mathbf{r}_2)\mathbf{k}^2 + \mathbf{k}'^2\delta(\mathbf{r}_1-\mathbf{r}_2)] + t_2(1+x_2P_\sigma)\mathbf{k}'.\delta(\mathbf{r}_1-\mathbf{r}_2)\mathbf{k}' + \cdots, \quad (22)$$

where we have set

$$t_0 = v_0,\ t_0x_0 = v_\sigma, \quad (23)$$

$$t_1 = -\frac{\mu^2}{2}v_0,\ t_1x_1 = -\frac{\mu^2}{2}v_\sigma, \quad (24)$$

$$t_2 = \frac{\mu^2}{2}v_0,\ t_2x_2 = \frac{\mu^2}{2}v_\sigma. \quad (25)$$

These relationships on the one side between the Skyrme parameters and the parameters of the Gaussian and, on the other side, the evident similarities between Skyrme and EFT Hamiltonians is a useful guidance to understand how the low-density behavior can be correctly reproduced using the Gaussian interaction. For instance, starting from Eq. (12), the standard expression of the neutron matter energy is recovered by expanding the function F up to second order in (μk_F). This expression matches Eqs. (5) and (18) under the set of conditions:

$$C_0 = t_0(1-x_0) = v_0 - v_\sigma = \frac{4\pi\hbar^2}{m}a_s, \quad (26)$$

$$C_2 = t_1(1-x_1) = -\frac{\mu^2}{2}(v_0-v_\sigma) = \frac{2\pi\hbar^2}{m}r_e a_s^2, \quad (27)$$

$$C_2' = t_2(1+x_2) = \frac{\mu^2}{2}(v_0+v_\sigma) = \frac{4\pi\hbar^2}{m}a_p^3. \quad (28)$$

With these relations, the same energy is obtained at the Hartree-Fock level either using the EFT Lagrangian, the Skyrme Hamiltonian or the Gaussian interaction provided that the energy (12) is expanded up to second order in (μk_F).

There are several useful relations that could be derived for the Gaussian interaction when the low-density limit is imposed. For instance, we have

$$\mu^2 = -2\frac{C_2}{C_0} = -(r_e a_s).$$

We then also get that the two parameters A and B entering in Eq. (12), respectively, write

$$A = -\frac{2\hbar^2\pi}{\nu m\mu^2}\left[(\nu-1)r_e a_s^2 - 2(\nu+1)a_p^3\right],$$

$$B = +\frac{2\hbar^2\pi}{\nu m\mu^2}\left[(\nu-1)r_e a_s^2 + 2(\nu+1)a_p^3\right].$$

C. Resummation of effective-range effect in Hartree-Fock theory

One motivation of the introduction of a finite-range interaction instead of a zero-range ansatz is the possibility to explore the effect of higher powers of the effective range, at least in the Hartree-Fock energy. For instance, Eq. (12) contains all powers in (μk_F). Our objective here is to show that the approximation (3) can be inferred from the Gaussian interaction case.

Starting from (12) and using the Taylor expansion of F, we deduce

$$\frac{E_G^{(1)}}{N} \simeq \frac{\rho}{2}\left[A - B\left\{1 - \frac{3}{10}(\mu k_F)^2\right\}\right], \simeq \frac{\rho}{2}\left[A - \frac{B}{1+\frac{3}{10}(\mu k_F)^2}\right]. \quad (29)$$

For simplicity, we now set the p-wave scattering volume to zero. In this case, we have

$$\frac{\rho}{2}A = -\frac{\rho}{2}B = \left(\frac{E_{\rm FG}}{N}\right)\frac{5}{9\pi}(\nu-1)(k_F a_s). \quad (30)$$

[3] Note that here we use a slightly different notation compared to standard definition. Indeed, the p-wave scattering volume α_p is usually defined though the $l=1$ phase shift using

$$\lim_{k\to 0} k^3\cot(\delta_1) = -\frac{1}{\alpha_p}. \quad (20)$$

We use here $\alpha_p = a_p^3$ so that a_p has a length unit.

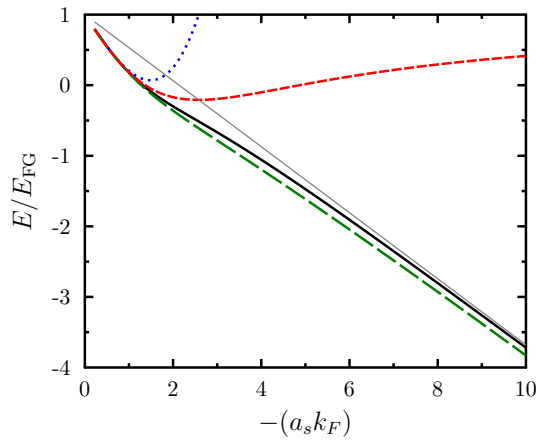

FIG. 3. $E/E_{\rm FG}$ as a function of $-(ak_F)$ obtained for a Gaussian interaction. The thick black solid line corresponds to Eq. (12) where A and B are calculated from the low-energy constant (with $a_p^3 = 0$). Note that the energy E corresponds to the sum of the kinetic and Hartree-Fock energy. The blue dotted line stands for the expansion (5) result, while the green long dashed line is obtained by using Eq. (31). The red short dashed line is obtained by using the alternative Eq. (32). The thin solid gray line is the function $1 + 5/(9\pi)(a_s k_F)$ that is shown for reference.

Then, using the value of μ, we deduce

$$\frac{E_G^{(1)}}{E_{\rm FG}} = \left(\frac{5}{9\pi}\right)[\nu - 1](a_s k_F)\left\{1 + \frac{1}{1 - \frac{3}{10}(a_s k_F)(r_e k_F)}\right\}. \tag{31}$$

In Fig. 3, the equivalent of the ξ parameter, Eq. (2), obtained for the Hartree-Fock energy of a Gaussian interaction is shown. In this figure, it is compared to the expansion (5) and to the result of (31). Obviously, Eq. (5) can only grasp the low-density regime of the HF energy. When using Eq. (31), the low-density limit is well reproduced. This finding has strongly guided the form of the functional proposed in Ref. [37]. Because the approximate form essentially mimics the effect of higher powers in $(r_e k_F)$, it can be interpreted as a resummed formula of the effective range for the Hartree-Fock energy. In particular, it is expected to have the correct limit at high density. We see, however, that it converges slower than the exact case to the energy $(\frac{5}{9\pi})[\nu - 1](a_s k_F)$. The faster convergence in the exact Hartree-Fock stems from the Gaussian that appears in Eq. (15). Alternative resummed expressions of effective-range effects are underway [55].

Our ultimate goal was, however, not to reproduce the Hartree-Fock energy of a finite-range interaction but to obtain a functional that has the proper low-density limit and a finite value at unitarity. This is not the case for the functional (31). However, resummation can be slightly modified to give

$$\frac{E_G^{(1)}}{N} \simeq \frac{\rho_0}{2}\frac{[A - B]}{1 - \frac{3B}{10[A-B]}(\mu k_F)^2}. \tag{32}$$

If we impose to reproduce the low-density limit, we get

$$\frac{\rho}{2}[A - B] = \left(\frac{E_{\rm FG}}{N}\right)\frac{10}{9\pi}(\nu - 1)(k_F a_s), \tag{33}$$

together with

$$\frac{B(\mu k_F)^2}{[A - B]} = \left[\frac{1}{2}(a_s k_F)(r_e k_F) + \left(\frac{\nu + 1}{\nu - 1}\right)\frac{(a_p k_F)^3}{(a_s k_F)}\right]. \tag{34}$$

To make contact with Eq. (3), we set to zero the p-wave scattering volume and then obtain

$$\frac{E_G^{(1)}}{E_{\rm FG}} = \left(\frac{10}{9\pi}\right)\frac{[\nu - 1](a_s k_F)}{1 - \frac{3}{20}(a_s k_F)(r_e k_F)}. \tag{35}$$

We recognize the terms $5/3A_0$ and A_0^{-1}/A_2 obtained in Eq. (3) when imposing the low-density limit. Not surprisingly, the term A_1 is not present because it was introduced to resum effects beyond Hartree-Fock [41]. The result of Eq. (32) is shown by the short dashed line in Fig. 3. By construction, it now goes to a finite value at large $-(a_s k_F)$ while the low-density behavior is preserved. Note that the fact we do not reproduce the exact Hartree-Fock result (for the Gaussian interaction) is not an issue because our ultimate goal is to treat the energy of a highly correlated system at large scattering length.

The Gaussian example gives some phenomenological insight on how the functional was originally guessed. The term A_1 contains in some effective way many-body effects beyond Hartree-Fock while the term A_2 contains effective-range effects, both terms being interpreted as resummation of complex many-body diagrams to all orders. From the present discussion, it is also clear that the specific formula used to include effective-range effect is not unique. Below, we will show that an alternative formula can improve the density functional at higher densities.

D. Inclusion of p-wave scattering volume effect in the functional

Our aim is now to improve the functional (7) by including possible p-wave effects. Let us first estimate the p-wave scattering volume relevant for neutron matter. Two neutrons can interact through $^3P_0$, $^3P_1$, and $^3P_2$. p-wave scattering volume estimates for each of these channels can be found in Refs. [56–58]. We retain here the values for neutron-neutron scattering:

$$\begin{aligned} a_0^3 &\simeq -2.45\ \text{fm}^3, \\ a_1^3 &\simeq 1.50\ \text{fm}^3, \\ a_2^3 &\simeq -0.29\ \text{fm}^3. \end{aligned} \tag{36}$$

Here a_i^3 denote the p-wave scattering volume in the channel ^3P_i. Accounting for the fact that these channels have, respectively, 1, 3, and 5 spin projection, the average p-wave scattering volume in neutron matter can be estimated through the weighted average:

$$a_p^3 = \tfrac{1}{9}\left(a_0^3 + 3a_1^3 + 5a_2^3\right), \tag{37}$$

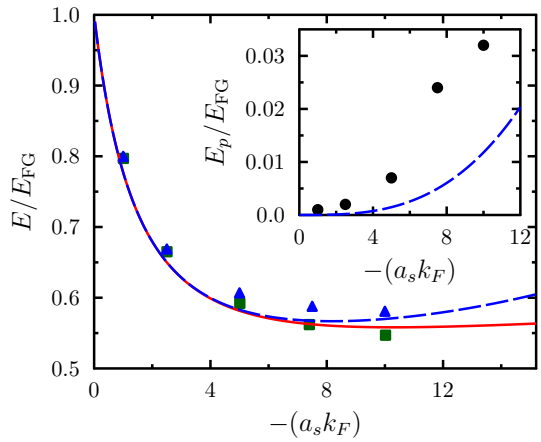

FIG. 4. Energy of neutron matter obtained in QMC calculations retaining only the s-wave contribution (green squares) or using the full AV4 interaction (blue triangle). The red solid corresponds to the result of the functional (7) without the p-wave contribution. The blue long-dashed line is obtained by adding the p-wave contribution using $a_p^3 = 0.25$ fm^3. In the inset, the blue long-dashed line represents the p-wave term of Eq. (5), i.e., $E_p/E_{\rm FG} = (\nu+1)(a_p k_F)^3/(3\pi)$ using $a_p^3 = 0.25$ fm^3. This term is compared to the difference between the energy obtained in QMC with AV4 and the QMC result with s-wave only (black solid circles).

leading to $a_p^3 \simeq 0.6$ fm^3. In particular, we see that we have the hierarchy of scales $a_s \gg r_e > a_p$. Note that the value of the scattering volume given above is directly extracted from experimental observation. It, however, differs from the p-wave scattering volume directly deduced for the AV4 interaction that was used in the QMC approach. For this simplified nuclear interaction, the three channels $^3P_0$, $^3P_1$, and $^3P_2$ are degenerate and have a scattering volume equal to 0.25 fm^3. Although 0.6 fm^3 seems more appropriate for nuclear systems, when comparing to QMC, the value 0.25 fm^3 is more meaningful.

For the range of $(a_s k_F)$ considered in Fig. 1(c), we have $(a_p k_F)$ much smaller than one. Therefore, we anticipate that the third term of Eq. (5) can eventually account for the p-wave contribution for this density range. In Fig. 4, we compare the QMC result obtained with full AV4 interaction in neutron matter [47] to the result obtained by simply adding to the functional (7) the p-wave term of Eq. (5) using $a_p^3 = 0.25$ fm^3. Similarly to the QMC calculation, we observe a global increase of the energy per particle. However, we see that the p-wave term leads to a slightly lower energy compared to QMC. This is illustrated in the inset of Fig. 4. The observed difference might be because of the necessity to add higher multipole contributions or to go beyond the leading order contribution for the p-wave in particular by treating interference terms with the s-wave channels that appear, for instance, from beyond mean-field effects.

IV. DISCUSSION OF EDF FOR NUCLEAR SYSTEM FROM LOW TO SATURATION DENSITY

Following Ref. [37], we are here proposing an EDF for neutron matter where parameters are determined either from the low-energy constant of the interaction or from the unitary limit. The simplest example of such functional is the Lee-Yang formula with increasing numbers of terms [46]. Unfortunately, because of the large s-wave scattering length, such an approach is restricted to very limited range of density, $\rho \leqslant 10^{-6}$ fm^{-3} that is several orders of magnitude smaller than the saturation density in nuclei. We introduce here a functional [Eq. (7)] that seems to be appropriate at much higher density $\rho \leqslant 0.01$ fm^{-3}. This is still rather small but we have gained several orders of magnitudes. Although the functional does not treat the nuclear many-body problem in its full complexity and is at this stage restricted to small densities, we will show that it can bring interesting insight on standard functionals used currently in nuclear physics.

One striking aspect in EDF is the apparent simplicity and remarkable predictive power of Skyrme-based EDF. The essence of Skyrme functionals is the use of a contact interaction where the t_0, t_1, and t_2 terms can be regarded as the s-wave, effective-range, and p-wave terms usually introduced in EFT (see discussion in Sec. III B). However, as underlined in Ref. [59], starting from Skyrme parameters, one can estimate the equivalent values of "Skyrme LEC," that we will denote below $a_s^{\rm Sk}$, $r_e^{\rm Sk}$, and $(a_p^{\rm Sk})^3$ using Eqs. (26)–(28). Deduced values have often nothing to do with physical values of nuclear LEC (see below). For instance, one typically obtains $|a_s| \equiv 1-5$ fm, that is much smaller than the expected 18.9-fm value. Here, we would like to show that the functional we propose might be useful (i) to understand why a simple functional like Skyrme EDF works so well and (ii) why the equivalent LEC differs so much from the physical ones.

Omitting the density-dependent and spin-orbit term, the Skyrme EDF mean-field energy can be written as the LO energy in EFT that is given by Eq. (18), provided that we use Eqs. (26)–(28). Starting from our new functional and to make contact with Skyrme or EFT, we introduce the three density-dependent terms $\widetilde{C}_0(k_F)$, $\widetilde{C}_2(k_F)$, and $\widetilde{C}_2'(k_F)$ and rewrite our functional as

$$\frac{E}{E_{\rm FG}} = 1 + \frac{k_F^3}{4\pi^2 E_{\rm FG}}\left\{\frac{\widetilde{C}_0(k_F)}{3} + \frac{k_F^2}{10}[(\nu-1)\widetilde{C}_2(k_F) + (\nu+1)\widetilde{C}_2'(k_F)]\right\}. \quad (38)$$

$\widetilde{C}_2(k_F)$ and $\widetilde{C}_2'(k_F)$ contains the term proportional to the effective range and p-wave scattering volume, respectively, while $\widetilde{C}_0(k_F)$ contains the rest. We then introduce density-dependent parameters $\widetilde{a}_s(k_F)$, $\widetilde{r}_e(k_F)$, and $\widetilde{a}_p^3(k_F)$ that are linked to the parameters $\widetilde{C}_{0,2}(k_F)$ and $\widetilde{C}_2'(k_F)$ through relations equivalent to (26)–(28). Then, the energy identifies with the expression (5), where the LEC are replaced by the new density-dependent parameters.

With these definitions, the density-dependent parameters can be expressed as a function of the parameters of the functional as

$$\widetilde{a}_s(k_F) = -\frac{1}{k_F}\frac{U_1}{[1-(a_s k_F)^{-1}U_1]}, \quad (39)$$

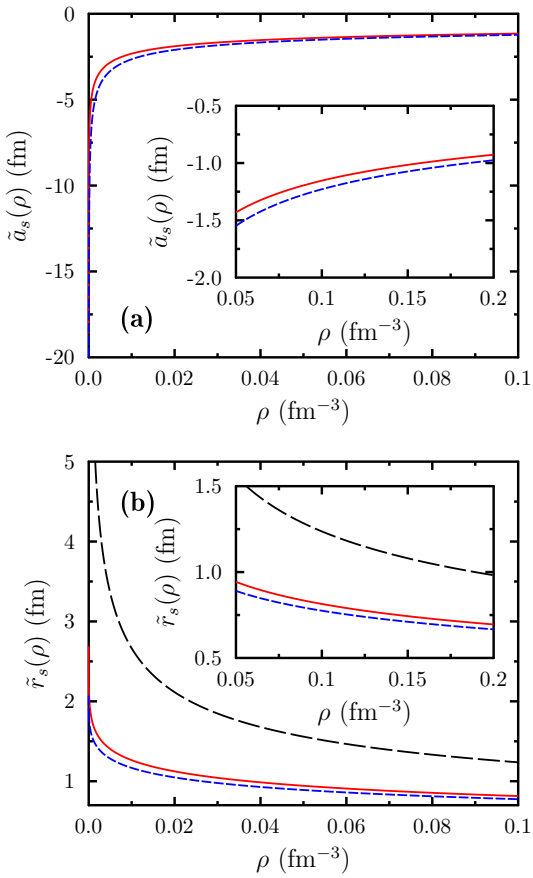

FIG. 5. The red solid lines give the evolution of the quantities (a) $\tilde{a}_s(\rho)$ and (b) $\tilde{r}_e(\rho)$ calculated through the expressions (39) and (40), respectively. The blue short dashed lines represent the approximate expressions (41) [(a)] and (42) [(b)]. In (b), the asymptotic limit at high density given by Eq. (43) is displayed by the black long-dashed line. In both panels, the insets focus on the density region $0.05\ \text{fm}^{-3} \leqslant \rho \leqslant 0.2\ \text{fm}^{-3}$.

and

$$\widetilde{r}_e(k_F) = \frac{1}{k_F^3 \widetilde{a}_s^2(k_F)} \times \frac{R_1^2(r_e k_F)}{[1 - R_1(a_s k_F)^{-1}][1 - R_1(a_s k_F)^{-1} + R_2(r_e k_F)]}. \tag{40}$$

Here the $U_i's$ and $R_i's$ are listed in Eq. (9). Note finally that we simply have here $\widetilde{a}_p = a_p$.

By construction, the constants $\widetilde{a}_s(k_F)$ and $\widetilde{r}_e(k_F)$ tend to the physical LEC at low density. The evolution of these quantities as a function of the density is shown in Fig. 5. In the limit of very large k_F, we can expand in $(a_s k_F)^{-1}$ and we obtain to leading order:

$$\widetilde{a}_s(k_F) \simeq -\frac{9\pi}{10 k_F}(1 - \xi_0), \tag{41}$$

$$\widetilde{r}_e(k_F) \simeq \frac{200}{27(\nu - 1)} \frac{\eta_e}{(1 - \xi_0)^2} \frac{r_e}{[1 + \delta_e(r_e k_F)/\eta_e]}. \tag{42}$$

It is worth mentioning that keeping these two terms in the energy, i.e., setting to zero the p-wave scattering volume, gives the unitary gas limit of the functional. Results of this functional are shown by the long dashed line in Fig. 1(c).

If we further take the LO in the expansion of $(r_e k_F)^{-1}$ in Eq. (42) we deduce for the asymptotic equation:

$$\widetilde{r}_e(k_F) \simeq \frac{200}{27(\nu - 1)} \frac{\eta_e^2}{(1 - \xi_0)^2 \delta_e k_F}. \tag{43}$$

There are several interesting conclusions one can draw from Fig. 5.

We can see two regimes of evolution of $\tilde{a}_s(\rho)$ and $\tilde{r}_e(\rho)$, first at very low density, they evolve very fast to much lower absolute values compared to their bare values. Then, they present a much smoother evolution towards higher densities. The sharp decrease is because of the strong influence of $-(a_s k_F)$ terms at very low density that tends rapidly to zero because of the very large value of a_s. This is illustrated by comparing the complete evolution (solid line) with the LO order in the expansion of $-(a_s k_F)^{-1}$ (short dashed line).

Strictly speaking, the present functional was validated up to densities $\rho < 0.01\ \text{fm}^{-1}$. The approximate expressions (41) and (42) are already very accurate. In addition, already at these densities, the effective values of the s-wave scattering length and effective range are strongly reduced compared to -18.9 fm and 2.7 fm.

One of the most surprising conclusions one can draw from the present analysis is that the s-wave scattering length has completely disappeared from the expressions (41) and (42). In particular, $\tilde{a}_s(\rho)$ has become independent of its value in the vacuum and its value is solely determined by the universal unitary gas parameters. This gives in particular an explanation why the parameters used to reproduce nuclear systems at equilibrium differ completely from those valid at low density [59].

It is worth mentioning that the expression (43) where both a_s and r_e have disappeared does not reproduce the full expression while the approximate form (42) provides a good approximation for densities $\rho \geqslant 0.1\ \text{fm}^{-3}$. Therefore, the connection of $\tilde{r}_e$ to r_e partially persists.

When the energy density functional becomes independent of the scale a_s at higher densities, the evolution of $\tilde{a}_s(\rho)$ and $\tilde{r}_e(\rho)$ is much slower. For instance, when the density increases from 0.01 fm^{-3} to 0.2 fm^{-3}, which are the densities of typical relevance for nuclear systems, we have

$$\begin{cases} -2.3\ \text{fm} \leqslant \tilde{a}_s(\rho) \leqslant -0.92\ \text{fm}, \\ +0.69\ \text{fm} \leqslant \tilde{r}_e(\rho) \leqslant +1.26\ \text{fm}. \end{cases} \tag{44}$$

These values can then be compared to the equivalent values obtained using the Skyrme functional. The equivalent values of the s-wave scattering length, effective range, and p-wave scattering volume, denoted, respectively, by a_s^{Sk}, r_e^{Sk}, and $(a_p^{\text{Sk}})^3$ can be obtained using the three equations (26)–(28) where the t_i and x_i parameters are the standard Skyrme parameters. Several examples obtained with different sets of Skyrme parameters are illustrated in Fig. 6. We see that the windows given in (44) are of the same order of magnitude compared to the Skyrme values. We also give in Fig. 6(c) the

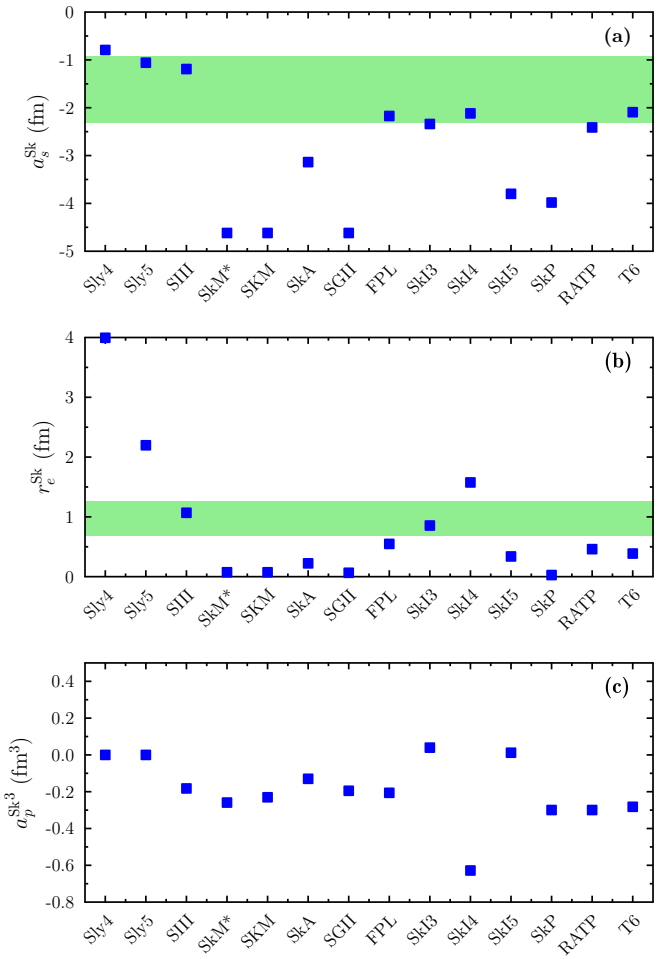

FIG. 6. Values of the quantities (a) $a_s^{\rm Sk}$ and (b) $r_e^{\rm Sk}$, for different widely used sets of Skyrme interaction parameters. In (a) and (b), the green area corresponds to the two windows of $\tilde{a}_s(\rho)$ and $\tilde{r}_e(\rho)$ values given by (44). For completeness we also give in (c) the equivalent to the p-wave scattering volume values $a_p^{\rm Sk^3}$ for the same set of Skyrme parameters.

equivalent p-wave scattering volume for Skyrme forces. We see that this volume is often negative and does not match the value relevant at low density, i.e., $a_p^3 = 0.6$ fm^3. This suggests that a treatment equivalent to what was done in the s wave should also be made for the p wave. We should, however, keep in mind that Skyrme functionals are globally adjusted and the physical interpretation of each separate term as coming from a single channel is *a priori* impossible, thus $(a_p^{\rm Sk})^3$ could receive contributions from higher partial waves (such as d waves) as well.

As a side remark, one could note that, within our approach, neither $\widetilde{C}_0(k_F)$ nor $\widetilde{C}_2(k_F)$ are constant parameters contrary to parameters in Skyrme functionals. The fact that latter functionals work so well might stem from the slow variations observed in the insets of Fig. 5.

The close agreement between the order of magnitude of the length (i.e., a_s, r_e) obtained in the new functional proposed here and the one deduced from Skyrme parameters is, to our opinion, a very interesting outcome of the present study. Indeed, sbecause Skyrme or other functionals are adjusted directly on expected properties in infinite systems or on experimental observation in finite systems, we *a priori* lose track of the underlying fundamental constants directly linked to the interaction or unitary limit. The present finding, however, opens up new hopes to get functionals close to the simple Skyrme ones built on first principles.

V. POSSIBLE EXTENSION OF THE FUNCTIONAL FROM LOW DENSITY TO SATURATION DENSITY

The functional (7) seems appropriate from very low density up to $\rho \equiv 0.01$ fm^{-3} [see Figs. 1(c) and 1(d)]. If we assume that the unitary gas limit is an adequate starting point (long-dashed line in Fig. 1), the discrepancy observed with our new functional and the *ab initio* calculations at higher densities might be from (i) the effects of higher partial waves of the two-body interaction; (ii) possible three-body interaction effects; (iii) the shape of the functional itself and in particular a too strong effect of r_e at high density.

Here, we explore the possibility of slightly modifying the r_e dependence such that the unitary and low density limit is still properly described while better reproducing *ab initio* results for $\rho > 0.01$ fm^{-3}. As shown in Sec. III C, the functional form is strongly guided by the resummation of the r_e effect for Hartree-Fock energy obtained with a finite-range interaction. More precisely, we used the approximation,

$$F(x) \simeq \frac{1}{1+\frac{3}{10}x^2}, \tag{45}$$

where $F(x)$ is given by Eq. (15). The resummed expression is designed such that the Taylor expansion up to $(\mu k_F)^2$ is the same and that the approximate functional remains close to the exact F at larger x values. Obviously, the function used for resummation is not unique and an alternative form can be used. In particular, as discussed from Fig. 3, the convergence towards the limit $1+\frac{5}{9\pi}(a_s k_F)$ is faster in the exact case, because of the Gaussian appearing in the F function given by Eq. (15). Another functional with improved property and that keeps the form Eq. (45) as a starting point can be simply obtained by using

$$\begin{aligned} F(x) &\simeq 1 - \frac{3}{10}x^2 + \frac{9}{140}x^4 + \cdots \\ &\simeq \frac{1}{1+\frac{3}{10}x^2} e^{-\alpha x^4}, \end{aligned}$$

with $\alpha = 9/350$. Such generalized expression improves slightly the approximate energy evolution compared to the exact HF one especially at large k_F. Again, this illustration can only give us a guidance to modify our functional because we are dealing here with strongly interacting systems.

Based on this simple example, the simplest way to reduce the effect of r_e in the functional (7) while keeping all the nice properties unchanged is to multiply the second term in Eq. (7) by $e^{-c(a_s/r_e)(r_e k_F)^4}$. Here $c(a_s/r_e)$ is a new parameter that should *a priori* be fixed with appropriate arguments. For instance, in the example given above, using the fact that $x = (a_s r_e k_F^2)$, we deduce $c(a_s/r_e) \simeq 0.026(a_s/r_e)^2$.

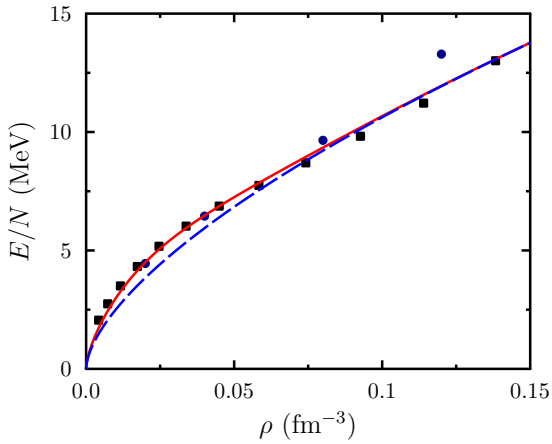

FIG. 7. Same as Fig. 1(d). The red solid line represents the result of the functional with the extra factor $e^{-c(r_e k_F)^4}$ in the r_e dependence.

There are arguments to assume that the c parameter should be independent of a_s for large densities. The first one is very practical. Indeed, if we suppose that this parameter is proportional to a_s^2, it will cancel the r_e dependence at unitarity and we cannot impose anymore the constraint (8). The second argument, more fundamental, stems from our previous conclusion that at densities above 0.01 fm^{-3}, the scales a_s become irrelevant. At this stage, we simply assume that c is a constant that is independent of a_s and should *a priori* be obtained from the unitary gas properties. Its determination would require one to have an extra term in the expansion (8). Because we do not have it, and as a proof of principle, we simply adjust this term to reproduce the *ab initio* result of Ref. [49] up to density $\rho = 0.16$ fm^{-3}. Doing so, we leave our original strategy to have no free parameters, hoping that future progress on unitary gas with effective range will justify the retained value of c. In Fig. 7 we show the result obtained with $c = 0.02$, keeping all parameters of the functional equals to their previous values given in the set of Eq. (9). We see in particular, as expected, that the low–density regime is still perfectly reproduced while a much better agreement is obtained at high density.

VI. SUMMARY AND DISCUSSION

In the present article, following the work of Ref. [37], we further discuss the possibility of developing nuclear DFT using the unitary regime as a starting point. One of the clear advantages of the present approach is that the functional has no free parameters and depends explicitly on the physical low-energy constant as well as on the universal parameters describing Fermi systems at unitarity. Several aspects of the functional proposed in Ref. [37] are clarified. We show that the good matching of the functional with the exact QMC approach illustrates that nuclear systems can be treated perturbatively in $-(a_s k_F)^{-1}$ with respect to the unitary gas.

An important advantage of the present approach compared to other functionals based on bare LEC like Lee-Yang EDF, is that it can be applied for densities that start to be of relevance for nuclear systems. By defining density-dependent scattering length and effective range, we analyze how these quantities make a transition from the very low density regime to higher densities. We show that the relevant scales are strongly renormalized at very low density. This rapid evolution stems from the anomalously large s-wave scattering length in nuclear systems. After this rapid evolution, the relevant scales stabilize and slowly evolve. An important conclusion we draw is that the smooth evolution is completely dominated by the universal constant at unitarity for the s wave. In particular, this scale becomes independent of its bare value. The situation is slightly different for the effective range. Its evolution depends on both the unitary regime and its bare limit r_e. Because the s-wave scattering length is the only scale that is anomalously large, we do anticipate that the behavior observed for the effective range should be the same for other scales in other channels.

One of the interesting byproducts of the present work is that it gives some preliminary steps towards explaining why simple functionals, like Skyrme functionals, can be so successful while the apparent associated scales completely differ from the physical ones at low densities. At the heart of the reasoning is that the part of the scales important in nuclear physics is not the one at this regime but the one at unitarity and therefore is independent of the underlying interaction.

A key aspect of the present work is the useful recent progress made on nuclear interactions, the precise study of systems at unitarity, and the possibility of obtaining exact solutions for nuclear systems and/or cold atoms in different regimes of s-wave scattering length. While the strategy we used here to design a nuclear DFT without any adjustable parameter is unambiguous, we are still far from having a predictive functional for densities up to twice the saturation density. Indeed, up to now we concentrated our attention to the neutron matter and incorporated essentially the s- and p-wave channels that are dominant at low density. To further progress, other states of matter with various spin and isospin contents should be considered together with higher order partial waves.

In the present exploratory study, the functional is solely designed for neutron systems. This restricts the range of applicability to neutron matter. One could also envisage the description of neutron droplets using, for instance, the local density approximation to treat finite systems. Work is in progress along this line. A great challenge to render the approach more versatile would be to extend it to nuclear matter and more generally to asymmetric matter. It should be noted that this project should be made back-to-back with progress in *ab initio* calculations, like QMC theory, to obtain exact benchmark calculations of increasing complexity including the effect beyond direct two-body interactions.

ACKNOWLEDGMENTS

The authors thank A. Gezerlis for useful discussion at different stages of the work and for providing a crosscheck of the p-wave scattering volume for the AV4 interaction. This project has received funding from the European Union Horizon 2020 research and innovation program under Grant No. 654002.

[1] D. Vautherin and D. M. Brink, Phys. Rev. C **5**, 626 (1972).
[2] D. Gogny, Nucl. Phys. A **237**, 399 (1975).
[3] D. Gogny, in *Proceedings of the International Conference on Nuclear Self-consistent Fields, Trieste 1975*, edited by G. Ripka and M. Porneuf (North-Holland, Amsterdam, 1975), pp. 176, 209, 265, 266.
[4] M. Bender *et al.*, Rev. Mod. Phys. **75**, 121 (2003).
[5] J. R. Stone and P.-G. Reinhard, Prog. Part. Nucl. Phys. **58**, 587 (2007).
[6] C. Simenel, D. Lacroix, and B. Avez, *Quantum Many-Body Dynamics: Applications to Nuclear Reactions* (VDM Verlag, Sarrebruck, 2010).
[7] T. Nakatsukasa, K. Matsuyanagi, M. Matsuo, and K. Yabana, Rev. Mod. Phys. **88**, 045004 (2016).
[8] M. Oertel, M. Hempel, T. Klähn, and S. Typel, Rev. Mod. Phys. **89**, 015007 (2017).
[9] E. Epelbaum, H.-W. Hammer, and U.-G. Meissner, Rev. Mod. Phys. **81**, 1773 (2009).
[10] T. T. S. Kuo, J. W. Holt, and E. Osnes, Phys. Scr. **91**, 033009 (2016).
[11] P. F. Bedaque and B. van Kolck, Annu. Rev. Nucl. Part. Sci. **52**, 339 (2002).
[12] J. W. Holt, N. Kaiser, and W. Weise, Prog. Part. Nucl. Phys. **73**, 35 (2013).
[13] A. Gezerlis, I. Tews, E. Epelbaum, S. Gandolfi, K. Hebeler, A. Nogga, and A. Schwenk, Phys. Rev. Lett. **111**, 032501 (2013).
[14] A. Gezerlis, I. Tews, E. Epelbaum, M. Freunek, S. Gandolfi, K. Hebeler, A. Nogga, and A. Schwenk, Phys. Rev. C **90**, 054323 (2014).
[15] E. Epelbaum, H. Krebs, and U.-G. Meissner, Eur. Phys. J. A **51**, 53 (2015).
[16] R. Machleidt and F. Sammarruca, Phys. Scr. **91**, 083007 (2016).
[17] U.-G. Meissner, Phys. Scr. **91**, 033005 (2016).
[18] S. Gandolfi, A. Gezerlis, and J. Carlson, Annu. Rev. Nucl. Part. Sci. **65**, 303 (2015).
[19] G. Hagen, M. Hjorth-Jensen, G. R. Jansen, and T. Papenbrock, Phys. Scr. **91**, 063006 (2016).
[20] P. Navrátil, S. Quaglioni, G. Hupin, C. Romero-Redondo, and A. Calci, Phys. Scr. **91**, 053002 (2016).
[21] C. Drischler, A. Carbone, K. Hebeler, and A. Schwenk, Phys. Rev. C **94**, 054307 (2016).
[22] J. Negele and D. Vautherin, Phys. Rev. C **5**, 1472 (1972).
[23] B. Gebremariam, T. Duguet, and S. K. Bogner, Phys. Rev. C **82**, 014305 (2010).
[24] M. Stoitsov, M. Kortelainen, S. K. Bogner, T. Duguet, R. J. Furnstahl, B. Gebremariam, and N. Schunck, Phys. Rev. C **82**, 054307 (2010).
[25] J. Dobaczewski, B. G. Carlsson, and M. Kortelainen, J. Phys. G: Nucl. Part. Phys. **37**, 075106 (2010).
[26] B. G. Carlsson and J. Dobaczewski, Phys. Rev. Lett. **105**, 122501 (2010).
[27] A. Dyhdalo, S. K. Bogner, and R. J. Furnstahl, arXiv:1611.03849 [Phys. Rev. C (to be published)].
[28] K. Moghrabi, M. Grasso, G. Colò, and N. Van Giai, Phys. Rev. Lett. **105**, 262501 (2010).
[29] N. Kaiser, J. Phys. G: Nucl. Part. Phys. **42**, 095111 (2015).
[30] C. J. Yang, M. Grasso, X. Roca-Maza, G. Colò, and K. Moghrabi, Phys. Rev. C **94**, 034311 (2016).
[31] S. Giorgini, L. P. Pitaevskii, and S. Stringari, Rev. Mod. Phys. **80**, 1215 (2008).
[32] I. Bloch, J. Dalibard, and W. Zwerger, Rev. Mod. Phys. **80**, 885 (2008).
[33] Edited by W. Zwerger, *The BCS-BEC Crossover and the Unitary Fermi Gas* (Springer Science and Business Media, Medford, 2011), Vol. 836.
[34] G. F. Bertsch, in *Recent Progress in Many-Body Theories*, edited by R. Bishop, K. A. Gernoth, N. R. Walet, and Y. Xian (World Scientific, Seattle, 2000).
[35] T. Papenbrock, Phys. Rev. A **72**, 041603(R) (2005).
[36] A. Bulgac, Phys. Rev. A **76**, 040502(R) (2007).
[37] D. Lacroix, Phys. Rev. A **94**, 043614 (2016).
[38] J. V. Steele, arXiv:cond-mat/0010066.
[39] T. Schäfer, C.-W. Kao, and S. R. Cotanch, Nucl. Phys. A **762**, 82 (2005).
[40] N. Kaiser, Nucl. Phys. A **860**, 41 (2011).
[41] C. J. Yang, M. Grasso, and D. Lacroix, Phys. Rev. C **94**, 031301(R) (2016).
[42] A. L. Fetter and J. D. Walecka, *Quantum Theory of Many-Particle Systems* (McGraw-Hill, New York, 1971).
[43] T. Papenbrock and G. F. Bertsch, Phys. Rev. C **59**, 2052 (1999).
[44] T. D. Lee and C. N. Yang, Phys. Rev. **105**, 1119 (1957).
[45] R. F. Bishop, Ann. Phys. **77**, 106 (1973).
[46] H. W. Hammer and R. J. Furnstahl, Nucl. Phys. A **678**, 277 (2000).
[47] A. Gezerlis and J. Carlson, Phys. Rev. C **81**, 025803 (2010).
[48] J. Carlson, S. Gandolfi, and A. Gezerlis, Prog. Theor. Exp. Phys. 01A209 (2012).
[49] B. Friedman and V. Pandharipande, Nucl. Phys. A **361**, 502 (1981).
[50] A. Akmal, V. R. Pandharipande, and D. G. Ravenhall, Phys. Rev. C **58**, 1804 (1998).
[51] M. McNeil Forbes, S. Gandolfi, and A. Gezerlis, Phys. Rev. A **86**, 053603 (2012).
[52] A. Bhattacharyya and T. Papenbrock, Phys. Rev. A **74**, 041602(R) (2006).
[53] S. K. Adhikari, Phys. Rev. A **77**, 045602 (2008).
[54] S. K. Adhikari and L. Salasnich, Phys. Rev. A **78**, 043616 (2008).
[55] A. Boulet and D. Lacroix (unpublished).
[56] R. B. Wiringa, V. G. J. Stoks, and R. Schiavilla, Phys. Rev. C **51**, 38 (1995).
[57] R. Machleidt, Phys. Rev. C **63**, 024001 (2001).
[58] M. Pavón Valderrama and E. Ruiz Arriola, arXiv:cond-mat/0407113.
[59] R. J. Furnstahl, in *Renormalization Group and Effective Field Theory Approaches to Many-Body Systems* (Springer, Berlin/Heidelberg, 2012), pp. 133–191.